Also available at http://amc.imfm.si
ISSN 1855-3966 (printed edn.), ISSN 1855-3974 (electronic edn.)
ARS MATHEMATICA CONTEMPORANEA 6 (2013) 221–236

Orienting and separating distance-transitive graphs

Ítalo J. Dejter
University of Puerto Rico, Rio Piedras, PR 00936-8377, Puerto Rico

Received 3 October 2011, accepted 7 March 2012, published online 6 September 2012

Abstract

It is shown that exactly 7 distance-transitive cubic graphs among the existing 12 possess a particular ultrahomogeneous property with respect to oriented cycles realizing the girth that allows the construction of a related Cayley digraph with similar ultrahomogeneous properties in which those oriented cycles appear minimally “pulled apart”, or “separated” and whose description is truly beautiful and insightful. This work is proposed as the initiation of a study of similar ultrahomogeneous properties for distance-transitive graphs in general with the aim of generalizing to constructions of similar related “separator” Cayley digraphs.

Keywords: Distance-transitive graph, ultrahomogeneous graph, Cayley graph.

Math. Subj. Class.: 05C62, 05B30, 05C20, 05C38

1 Introduction

A graph is said to be distance-transitive if its automorphism group acts transitively on ordered pairs of vertices at distance i, for each $i \geq 0$ [3, 10, 15]. In this paper we deal mainly with finite cubic distance-transitive graphs. While these graphs are classified and very well-understood since there are only twelve examples, for this very restricted class of graphs we investigate a property called ultrahomogeneity that plays a very important role in logic, see for example [7, 18]. For ultrahomogeneous graphs (resp. digraphs), we refer the reader to [5, 9, 11, 17, 19] (resp. [6, 8, 16]). Distance-transitive graphs and ultrahomogeneous graphs are very important and worthwhile to investigate. However, to start with, the following question is answered in the affirmative for 7 of the 12 existing cubic distance-transitive graphs G and negatively for the remaining 5:

Question 1.1. If k is the largest ℓ such that G is ℓ-arc-transitive, is it possible to orient all shortest cycles of G so that each two oppositely oriented $(k-1)$-arcs of G are just in two corresponding oriented shortest cycles?

E-mail address: ijdejter@uprrp.edu (Ítalo J. Dejter)

Copyright © 2013 DMFA Slovenije

The answer (below) to Question 1 leads to 7 connected digraphs $\mathcal{S}(G)$ in which all oriented shortest cycles of G are minimally "pulled apart" or "separated". Specifically, it is shown that all cubic distance-transitive graphs are $\{C_g\}_{P_k}$-ultrahomogeneous, where $g =$ girth, but only the 7 cited G are $\{\vec{C}_g\}_{\vec{P}_k}$-ultrahomogeneous digraphs and in each of these 7 digraphs G, the corresponding "separator" digraph $\mathcal{S}(G)$ is: **(a)** vertex-transitive digraph of indegree = outdegree = 2, underlying cubic graph and automorphism group as that of G; **(b)** $\{\vec{C}_g, \vec{C}_2\}$-ultrahomogeneous digraph, where $\vec{C}_g =$ induced oriented g-cycle, with each vertex taken as the intersection of exactly one such $\vec{C}_g$ and one $\vec{C}_2$; **(c)** a Cayley digraph. The structure and surface-embedding topology [2, 12, 20] of these $\mathcal{S}(G)$ are studied as well. We remark that the description of these $\mathcal{S}(G)$ is truly beautiful and insightful.

It remains to see how Question 1 can be generalized and treated for distance-transitive graphs of degree larger than 3 and what separator Cayley graphs could appear via such a generalization.

2 Preliminaries

We may consider a graph G as a digraph by taking each edge e of G as a pair of oppositely oriented (or O-O) arcs $\vec{e}$ and $(\vec{e})^{-1}$ inducing an oriented 2-cycle $\vec{C}_2$. Then, *fastening* $\vec{e}$ and $(\vec{e})^{-1}$ allows to obtain precisely the edge e in the graph G. Is it possible to orient all shortest cycles in a distance-transitive graph G so that each two O-O $(k-1)$-arcs of G are in just two oriented shortest cycles, where $k =$ largest ℓ such that G is ℓ-arc transitive? It is shown below that this is so just for 7 of the 12 cubic distance-transitive graphs G, leading to 7 corresponding minimum connected digraphs $\mathcal{S}(G)$ in which all oriented shortest cycles of G are "pulled apart" by means of a graph-theoretical operation explained in Section 4 below.

Given a collection $\mathcal{C}$ of (di)graphs closed under isomorphisms, a (di)graph G is said to be $\mathcal{C}$-*ultrahomogeneous* (or $\mathcal{C}$-UH) if every isomorphism between two induced members of $\mathcal{C}$ in G extends to an automorphism of G. If $\mathcal{C}$ is the isomorphism class of a (di)graph H, we say that such a G is $\{H\}$-UH or H-UH. In [14], $\mathcal{C}$-UH graphs are defined and studied when $\mathcal{C}$ is the collection of either the complete graphs, or the disjoint unions of complete graphs, or the complements of those unions.

Let M be an induced subgraph of a graph H and let G be both an M-UH and an H-UH graph. We say that G is an $\{H\}_M$-*UH graph* if, for each induced copy H_0 of H in G and for each induced copy M_0 of M in H_0, there exists exactly one induced copy $H_1 \neq H_0$ of H in G with $V(H_0) \cap V(H_1) = V(M_0)$ and $E(H_0) \cap E(H_1) = E(M_0)$. The vertex and edge conditions above can be condensed as $H_0 \cap H_1 = M_0$. We say that such a G is *tightly fastened*. This is generalized by saying that an $\{H\}_M$-UH graph G is an ℓ-*fastened* $\{H\}_M$-UH graph if given an induced copy H_0 of H in G and an induced copy M_0 of M in H_0, then there exist exactly ℓ induced copies $H_i \neq H_0$ of H in G such that $H_i \cap H_0 \supseteq M_0$, for each $i = 1, 2, \dots, \ell$, with at least $H_1 \cap H_0 = M_0$.

Let $\vec{M}$ be an induced subdigraph of a digraph $\vec{H}$ and let the graph G be both an $\vec{M}$-UH and an $\vec{H}$-UH digraph. We say that G is an $\{\vec{H}\}_{\vec{M}}$-*UH digraph* if for each induced copy $\vec{H}_0$ of $\vec{H}$ in $\vec{G}$ and for each induced copy $\vec{M}_0$ of $\vec{M}$ in $\vec{H}_0$ there exists exactly one induced copy

$\vec{H}_1 \neq \vec{H}_0$ of $\vec{H}$ in G with $V(\vec{H}_0) \cap V(\vec{H}_1) = V(\vec{M}_0)$ and $A(\vec{H}_0) \cap \bar{A}(\vec{H}_1) = A(\vec{M}_0)$, where $\bar{A}(\vec{H}_1)$ is formed by those arcs $(\vec{e})^{-1}$ whose orientations are reversed with respect to the orientations of the arcs $\vec{e}$ of $A(\vec{H}_1)$. Again, we say that such a G is *tightly fastened*. This case is used in the constructions of Section 4.

Given a finite graph H and a subgraph M of H with $|V(H)| > 3$, we say that a graph G is (*strongly fastened*) *SF* $\{H\}_M$-UH if there is a descending sequence of connected subgraphs $M = M_1, M_2 \ldots, M_t \equiv K_2$ such that: **(a)** M_{i+1} is obtained from M_i by the deletion of a vertex, for $i = 1, \ldots, t-1$ and **(b)** G is a $(2^i - 1)$-fastened $\{H\}_{M_i}$-UH graph, for $i = 1, \ldots, t$.

This paper deals with the above defined $\mathcal{C}$-UH concepts applied to cubic distance-transitive (CDT) graphs [3]. A list of them and their main parameters follows:

CDT graph G	n	d	g	k	η	a	b	h	κ
Tetrahedral graph K_4	4	1	3	2	4	24	0	1	1
Thomsen graph $K_{3,3}$	6	2	4	3	9	72	1	1	2
3-cube graph Q_3	8	3	4	2	6	48	1	1	1
Petersen graph	10	2	5	3	12	120	0	0	0
Heawood graph	14	3	6	4	28	336	1	1	0
Pappus graph	18	4	6	3	18	216	1	1	0
Dodecahedral graph	20	5	5	2	12	120	0	1	1
Desargues graph	20	5	6	3	20	240	1	1	3
Coxeter graph	28	4	7	3	24	336	0	0	3
Tutte 8-cage	30	4	8	5	90	1440	1	1	2
Foster graph	90	8	10	5	216	4320	1	1	0
Biggs-Smith graph	102	7	9	4	136	2448	0	1	0

where n = order; d = diameter; g = girth; k = AT or arc-transitivity (= largest ℓ such that G is ℓ-arc transitive); η = number of g-cycles; a = number of automorphisms; b (resp. h) = 1 if G is bipartite (resp. hamiltonian) and = 0 otherwise; and κ is defined as follows: let P_k and $\vec{P}_k$ be respectively a $(k-1)$-path and a directed $(k-1)$-path (of length $k-1$); let C_g and $\vec{C}_g$ be respectively a cycle and a directed cycle of length g; then (see Theorem 3 below): $\kappa = 0$, if G is not $(\vec{C}_g; \vec{P}_k)$-UH; $\kappa = 1$, if G is planar; $\kappa = 2$, if G is $\{\vec{C}_g\}_{\vec{P}_k}$-UH with $g = 2(k-1)$; $\kappa = 3$, if G is $\{\vec{C}_g\}_{\vec{P}_k}$-UH with $g > 2(k-1)$.

In Section 3 below, Theorem 2 proves that every CDT graph is an SF $\{C_g\}_{P_k}$-UH graph, while Theorem 3 establishes exactly which CDT graphs are not $\{\vec{C}_g\}_{\vec{P}_k}$-UH digraphs; in fact 5 of them. Section 4 shows that each of the remaining 7 CDT graphs G yields a digraph $\mathcal{S}(G)$ whose vertices are the $(k-1)$-arcs of G, an arc in $\mathcal{S}(G)$ between each two vertices representing corresponding $(k-1)$-arcs in a common oriented g-cycle of G and sharing just one $(k-2)$-arc; additional arcs of $\mathcal{S}(G)$ appearing in O-O pairs associated with the reversals of $(k-1)$-arcs of G. Moreover, Theorem 4 asserts that each $\mathcal{S}(G)$ is as claimed and itemized at end of the Introduction above.

3 (C_g, P_k)-UH properties of CDT graphs

Theorem 3.1. Let G be a CDT graph of girth $= g$, AT $= k$ and order $= n$. Then, G is an SF $\{C_g\}_{P_k}$-UH graph. In particular, G has exactly $2^{k-2}3ng^{-1}$ g-cycles.

Proof. We have to see that each CDT graph G with girth $= g$ and AT $= k$ is a $(2^{i+1}-1)$-fastened $\{C_g\}_{P_{k-i}}$-UH graph, for $i = 0,1,\dots,k-2$. In fact, each $(k-i-1)$-path $P = P_{k-i}$ of any such G is shared by exactly 2^{i+1} g-cycles of G, for $i = 0,1,\dots,k-2$. For example if $k = 4$, then any edge (resp. 2-path, resp. 3-path) of G is shared by 8 (resp. 4, resp. 2) g-cycles of G. This means that a g-cycle C_g of G shares a P_2 (resp. P_3, resp. P_4) with exactly other 7 (resp. 3, resp. 1) g-cycles. Thus G is an SF $\{C_g\}_{P_{i+2}}$-UH graph, for $i = 0,1,\dots,k-2$. The rest of the proof depends on the particular cases analyzed in the proof of Theorem 3 below and on some simple counting arguments for the pertaining numbers of g-cycles. □

Given a CDT graph G, there are just two g-cycles shared by each $(k-1)$-path. If in addition G is a $\{\vec{C}_g\}_{\vec{P}_k}$-UH graph, then there exists an assignment of an orientation for each g-cycle of G, so that the two g-cycles shared by each $(k-1)$-path receive opposite orientations. We say that such an assignment is a $\{\vec{C}_g\}_{\vec{P}_k}$*-O-O assignment* (or $\{\vec{C}_g\}_{\vec{P}_k}$-OOA). The collection of η oriented g-cycles corresponding to the η g-cycles of G, for a particular $\{\vec{C}_g\}_{\vec{P}_k}$-OOA will be called an $\{\eta\vec{C}_g\}_{\vec{P}_k}$-OOC. Each such g-cycle will be expressed with its successive composing vertices expressed between parentheses but without separating commas, (as is the case for arcs uv and 2-arcs uvw), where as usual the vertex that succeeds the last vertex of the cycle is its first vertex.

Theorem 3.2. The CDT graphs G of girth $= g$ and AT $= k$ that are not $\{\vec{C}_g\}_{\vec{P}_k}$-UH digraphs are the graphs of Petersen, Heawood, Pappus, Foster and Biggs-Smith. The remaining 7 CDT graphs are $\{\vec{C}_g\}_{\vec{P}_k}$-UH digraphs.

Proof. Let us consider the case of each CDT graph sequentially. The graph K_4 on vertex set $\{1,2,3,0\}$ admits the $\{4\,\vec{C}_3\}_{\vec{P}_2}$-OOC $\{(123),\ (210),(301),(032)\}$. The graph $K_{3,3}$ obtained from K_6 (with vertex set $\{1,2,3,4,5,0\}$) by deleting the edges of the triangles $(1,3,5)$ and $(2,4,0)$ admits the $\{9\,\vec{C}_4\}_{\vec{P}_3}$-OOC $\{(1234),\ (3210),\ (4325),\ (1430),\ (2145),\ (0125),\ (5230),\ (0345),\ (5410)\}$. The graph Q_3 with vertex set $\{0,\dots,7\}$ and edge set $\{01,23,45,67,02,13,46,57,04,15,26,37\}$ admits the $\{6\,\vec{C}_4\}_{\vec{P}_2}$-OOC $\{(0132),\ (1045),\ (3157),\ (2376),\ (0264),\ (4675)\}$.

The Petersen graph Pet is obtained from the disjoint union of the 5-cycles $\mu^\infty = (u_0u_1u_2\ u_3u_4)$ and $\nu^\infty = (v_0v_2v_4v_1v_3)$ by the addition of the edges (u_x,v_x), for $x \in \mathbf{Z}_5$. Apart from the two 5-cycles given above, the other 10 5-cycles of Pet can be denoted by $\mu^x = (u_{x-1}u_xu_{x+1}v_{x+1}v_{x-1})$ and $\nu^x = (v_{x-2}v_xv_{x+2}u_{x+2}u_{x-2})$, for each $x \in \mathbf{Z}_5$. Then, the following sequence of alternating 5-cycles and 2-arcs starts and ends up with opposite orientations:

$$\mu^2_- \quad u_3u_2u_1 \quad \mu^\infty_+ \quad u_0u_1u_2 \quad \mu^1_- \quad u_2v_2v_0 \quad \nu^0_- \quad v_3u_3u_2 \quad \mu^2_+,$$

where the subindexes $\pm$ indicate either a forward or backward selection of orientation and each 2-path is presented with the orientation of the previously cited 5-cycle but must be present in the next 5-cycle with its orientation reversed. Thus Pet cannot be a $\{\vec{C}_5\}_{\vec{P}_3}$-UH digraph.

Another way to see this is via the auxiliary table indicated below, that presents the form in which the 5-cycles above share the vertex sets of 2-arcs, either O-O or not. The table details, for each one of the 5-cycles $\xi = \mu^\infty, \nu^\infty, \mu^0, \nu^0$, (expressed as $\xi = (\xi_0,\dots,\xi_4)$ in the shown vertex notation), each 5-cycle η in $\{\mu^i,\nu^i; i=\infty,0,\dots,4\}\backslash\{\xi\}$ that intersects ξ in the succeeding 2-paths $\xi_i\xi_{i+1}\xi_{i+2}$, for $i=0,\dots,4$, with additions involving i taken mod 5. Each such η in the auxiliary table has either a preceding minus sign, if the corresponding 2-arcs in ξ and η are O-O, or a plus sign, otherwise. Each $-\eta_j$ (resp. η_j) shown in the table has the subindex j indicating the equality of initial vertices $\eta_j=\xi_{i+2}$ (resp. $\eta_j=\xi_i$) of those 2-arcs, for $i=0,\dots,4$:

$$\mu^\infty:(+\mu^1_0,+\mu^2_0,+\mu^3_0,+\mu^4_0,+\mu^0_0),\quad \nu^\infty:(+\nu^2_0,+\nu^4_0,+\nu^1_0,+\nu^3_0,+\nu^0_0),$$
$$\mu^0:(+\mu^\infty_4,+\nu^3_3,-\nu^4_1,-\nu^1_4,+\nu^2_2),\quad \nu^0:(+\nu^\infty_4,-\mu^1_2,+\mu^3_4,+\mu^2_1,-\mu^4_3).$$

This partial auxiliary table is extended to the whole auxiliary table by adding $x\in\mathbf{Z}_4$ uniformly mod 5 to all superindexes $\neq\infty$, reconfirming that Pet is not $\{\vec{C}_5\}_{\vec{P}_3}$-UH.

For each positive integer n, let I_n stand for the n-vertex cycle $(0,1,\dots,n-1)$. The Heawood graph Hea is obtained from I_{14} by adding the edges $(2x,5+2x)$, where $x\in\{1,\dots,7\}$ and operations are in $\mathbf{Z}_{14}$. The 28 6-cycles of Hea include the following 7 6-cycles:

$$\gamma^x=(2x,2x{+}1,2x{+}2,2x{+}3,2x{+}4,2x{+}5),\quad \delta^x=(2x,2x{+}5,2x{+}6,2x{+}7,2x{+}8,2x{+}13),$$
$$\epsilon^x=(2x,2x{+}5,2x{+}4,2x{+}9,2x{+}8,2x{+}13),\quad \zeta^x=(2x{+}12,2x{+}3,2x{+}4,2x{+}5,2x,2x{+}13),$$

where $x\in\mathbf{Z}_7$. Now, the following sequence of alternating 6-cycles and 3-arcs starts and ends with opposite orientations for γ_0:

$$\gamma^0_+\ 2345\ \gamma^1_-\ 7654\ \gamma^2_+\ 6789\ \gamma^3_-\ ba98\ \gamma^4_+\ abcd\ \gamma^5_-\ 10dc\ \gamma^6_+\ 0123\ \gamma^0_-,$$

(where tridecimal notation is used, up to $d=13$). Thus Hea cannot be a $\{\vec{C}_7\}_{\vec{P}_4}$-UH digraph. Another way to see this is via an auxiliary table for Hea obtained in a fashion similar to that of the one for Pet above from:

$$\gamma^0:(+\gamma^6_2,+\delta^5_1,+\gamma^1_0,+\zeta^6_1,-\epsilon^5_1,-\zeta^0_4);\quad \epsilon^0:(+\epsilon^5_2,-\gamma^2_4,+\epsilon^2_0,+\zeta^4_5,+\delta^0_4,-\zeta^6_2);$$
$$\delta^0:(+\zeta^0_0,+\gamma^2_1,-\zeta^3_3,+\delta^4_5,+\epsilon^0_4,+\delta^3_3);\quad \zeta^0:(+\delta^0_0,+\gamma^1_3,-\epsilon^1_5,-\delta^4_2,-\gamma^0_5,+\epsilon^3_3).$$

This reaffirms that Hea is not $\{\vec{C}_6\}_{\vec{P}_4}$-UH.

The Pappus graph Pap is obtained from I_{18} by adding to it the edges $(1+6x,6+6x)$, $(2+6x,9+6x)$, $(4+6x,11+6x)$, for $x\in\{0,1,2\}$, with sums and products taken mod 18. The 6-cycles of Pap are expressible as: $A_0=(123456)$, $B_0=(3210de)$, $C_0=(34bcde)$, $D_0=(165gh0)$, $E_0=(329ab4)$ (where octodecimal notation is used, up to $h=17$), the 6-cycles A_x,B_x,C_x,D_x,E_x obtained by uniformly adding $6x$ mod 18 to the vertices of A_0,B_0,C_0,D_0,E_0, for $x\in\mathbf{Z}_3\setminus\{0\}$, and $F_0=(3298fe)$, $F_1=(hg54ba)$, $F_2=(167cd0)$. No orientation assignment makes these cycles into an $\{18\,\vec{C}_6\}_{\vec{P}_3}$-OOC, for the following sequence of alternating 6-cycles and 2-arcs (with orientation reversed between each preceding 6-cycle to corresponding succeeding 6-cycle) reverses the orientation of its initial 6-cycle in its terminal one:

$$D_1^{-1}654\,A_0123\,B_0210\,C_1h01\,D_0^{-1}g56\,C_2^{-1}876\,B_1^{-1}789\,A_1^{-1}cba\,D_2abc\,A_1^{-1}987\,B_1^{-1}678\,C_2^{-1}765D_1$$
$$=(654bc7)\,654\,(123456)\,123\,(3210de)\,210\,(0129ah)\,h01\,(10hg56)\,g56\,(5gf876)\,876$$
$$(216789)\,789(cba987)\,cba(d0habc)\,abc(cba987)\,987\,(216789)\,678\,(5gf876)\,765(cb4567).$$

Another way to see this is via an auxiliary table for Pap obtained in a fashion similar to those above for Pet and Hea, where $x=0,1,2$ (mod 3):

$$-A_x:(B_x,E_x,E_{x+2},D_{x+1},D_x,B_{x+1});\quad -F_0:(E_0,B_1,E_1,B_2,E_2,B_0);$$
$$-B_x:(A_x,C_{x+1},F_2,A_{x+2},C_x,F_0);\quad -F_1:(D_0,E_2,D_1,E_0,D_2,E_1);$$
$$-C_x:(E_x,D_{x+1},D_{x+2},B_{x+2},B_x,E_{x+2});\quad -F_2:(B_1,D_1,B_2,D_2,B_0,D_0);$$
$$-D_x:(A_x,C_{x+2},F_1,A_{x+2},C_{x+1},F_2);$$
$$-E_x:(F_0,C_{x+1},A_{x+1},F_1,C_x,A_x).$$

This reaffirms that Pap is not a $\{\vec{C}_6\}_{\vec{P}_3}$-UH digraph. In fact, observe that any two 6-cycles here that share a 2-path possess the same orientation, in total contrast to what happens in the 7 cases that are being shown to be $\{\vec{C}_g\}_{\vec{P}_k}$-UH digraphs, in the course of this proof.

The Desargues graph Des is obtained from the 20-cycle I_{20}, with vertices $4x, 4x+1, 4x+2, 4x+3$ redenoted alternatively x_0, x_1, x_2, x_3, respectively, for $x \in \mathbf{Z}_5$, by adding the edges $(x_3, (x+2)_0)$ and $(x_1, (x+2)_2)$, where operations are mod 5. Then, Des admits a $\{20\,\vec{C}_6\}_{\vec{P}_3}$-OOC formed by the oriented 6-cycles A^x, B^x, C^x, D^x, for $x \in \{0, \ldots, 4\}$, where

$$A^x{=}(x_0x_1x_2x_3(x{+}1)_0(x{+}4)_3), \qquad B^x{=}(x_1x_0(x{+}4)_3(x{+}4)_2(x{+}2)_1(x{+}2)_2),$$
$$C^x{=}(x_2x_1x_0(x{+}3)_3(x{+}3)_2(x{+}3)_1), \qquad D^x{=}(x_0(x{+}4)_3(x{+}1)_0(x{+}1)_1(x{+}3)_2(x{+}3)_3).$$

The successive copies of $\vec{P}_3$ here, when reversed in each case, must belong to the following remaining oriented 6-cycles:

$$A^x{:}(C^x,C^{x+2},B^{x+1},D^{x+1},D^x,B^x); \qquad B^x{:}(A^x,A^{x+4},D^{x+1},C^{x+4},C^{x+2},D^{x+4});$$
$$C^x{:}(A^x,D^{x+4},D^x,A^{x+3},B^{x+1},B^{x+3}); \qquad D^x{:}(A^x,C^{x+1},B^{x+1},B^{x+4},C^x,A^{x+4});$$

showing that they constitute effectively an $\{\eta\vec{C}_g\}_{\vec{P}_k}$-OOC.

The dodecahedral graph Δ is a 2-covering graph of the Petersen graph H, where each vertex u_x, (resp., v_x), of H is covered by two vertices a_x, c_x, (resp. b_x, d_x). A $\{12\,\vec{C}_5\}_{\vec{P}_2}$-OOC of Δ is given by the oriented 5-cycles $(a_0a_1a_2a_3a_4)$, $(c_4c_3c_2c_1c_0)$ and, for each $x \in \mathbf{Z}_5$, also by $(a_xd_xb_{x-2}d_{x+1}a_{x+1})$ and $(d_xb_{x+2}c_{x+2}c_{x-2}b_{x-2})$.

The Tutte 8-cage Tut is obtained from I_{30}, with vertices $6x, 6x+1, 6x+2, 6x+3, 6x+4, 6x+5$ denoted alternatively $x_0, x_1, x_2, x_3, x_4, x_5$, respectively, for $x \in \mathbf{Z}_5$, by adding the edges $(x_5, (x+2)_0)$, $(x_1, (x+1)_4)$ and $(x_2, (x+2)_3)$. Then, Tut admits the $\{90\,\vec{C}_8\}_{\vec{P}_5}$-OOC formed by the oriented 8-cycles:

$$A^0{=}(4_50_00_10_20_30_40_51_0), \quad B^0{=}(4_24_34_44_51_01_11_21_3), \quad C^0{=}(0_20_30_44_14_02_52_42_3),$$
$$D^0{=}(3_33_23_14_44_34_21_31_2), \quad E^0{=}(4_51_00_50_44_14_03_50_0), \quad F^0{=}(4_50_03_54_02_52_41_11_0),$$
$$G^0{=}(1_01_12_42_30_20_10_04_5), \quad H^0{=}(2_32_41_11_00_50_40_30_2), \quad I^0{=}(0_10_20_30_44_14_21_31_4),$$
$$J^0{=}(1_00_50_40_33_23_14_44_5), \quad K^0{=}(3_13_20_30_20_10_04_54_4), \quad L^0{=}(2_32_42_53_03_13_20_30_2),$$
$$M^0{=}(3_54_04_10_40_30_20_10_0), \quad N^0{=}(0_00_11_41_52_02_13_43_5), \quad O^0{=}(4_24_32_22_13_43_31_21_3),$$
$$P^0{=}(4_54_44_34_24_10_40_51_0), \quad Q^0{=}(4_04_14_21_31_41_53_02_5), \quad R^0{=}(0_10_20_33_23_13_01_51_4),$$

together with those obtained by adding $y \in \mathbf{Z}_5$ uniformly mod 5 to all numbers x of vertices x_i in $A^0, \ldots, R^0$, for each $y = 1, 2, 3, 4$, yielding in each case oriented 8-cycles $A^y, \ldots, R^y$.

The Coxeter graph Cox is obtained from three 7-cycles $(u_1u_2u_3u_4u_5u_6u_0)$, $(v_4v_6v_1v_3v_5v_0v_2)$, $(t_3t_6t_2t_5t_1t_4t_0)$ by adding a copy of $K_{1,3}$ with degree-1 vertices u_x, v_x, t_x and a central degree-3 vertex z_x, for each $x \in \mathbf{Z}_7$. Cox admits the $\{24\,\vec{C}_7\}_{\vec{P}_3}$-OOC:

$$\{0^1{=}(u_1u_2u_3u_4u_5u_6u_0), \quad 0^2{=}(v_1v_3v_5v_0v_2v_4v_6), \quad 0^3{=}(t_1t_5t_2\,t_6\,t_3\,t_0\,t_4),$$
$$1^1{=}(u_1z_1v_1\,v_3\,z_3u_3u_2), \quad 1^2{=}(z_4v_4v_2v_0z_0\,t_0t_4), \quad 1^3{=}(t_6t_2t_5z_5u_5u_6z_6),$$
$$2^1{=}(v_5z_5u_5u_4u_3\,z_3\,v_3), \quad 2^2{=}(t_6z_6v_6v_4v_2\,z_2t_2), \quad 2^3{=}(u_1z_1t_1t_4t_0z_0u_0),$$
$$3^1{=}(v_5v_0z_0u_0u_6\,u_5\,z_5), \quad 3^2{=}(z_4t_4t_1z_1v_1\,v_6v_4), \quad 3^3{=}(t_6t_2z_2u_2u_3z_3t_3),$$
$$4^1{=}(u_1u_0z_0v_0v_2\,z_2\,u_2), \quad 4^2{=}(t_6t_3z_3v_3v_1v_6\,z_6), \quad 4^3{=}(z_4u_4u_5z_5t_5t_1t_4),$$
$$5^1{=}(z_4u_4u_3u_2z_2\,v_2\,v_4), \quad 5^2{=}(v_5v_3v_1z_1t_1t_5\,z_5), \quad 5^3{=}(t_6z_6u_6u_0z_0t_0t_3),$$
$$6^1{=}(z_4v_4v_6z_6u_6\,u_5\,u_4), \quad 6^2{=}(v_5v_3z_3t_3t_0\,z_0v_0), \quad 6^3{=}(u_1u_2z_2t_2t_5t_1z_1),$$
$$7^1{=}(u_1u_0u_6z_6v_6\,v_1\,z_1), \quad 7^2{=}(v_5z_5t_5t_2z_2\,v_2v_0), \quad 7^3{=}(z_4t_4t_0t_3z_3u_3u_4)\}.$$

The Foster graph Fos is obtained from I_{90}, with vertices $6x, 6x+1, 6x+2, 6x+3, 6x+4, 6x+5$ denoted alternatively x_0, x_1, x_2, x_3, x_4, x_5, respectively, for $x \in \mathbf{Z}_{15}$, by adding the edges $(x_4, (x+2)_1)$, $(x_0, (x+2)_5)$ and $(x_2, (x+6)_3)$. The 216 10-cycles of Fos include the following 15 10-cycles, where $x \in \mathbf{Z}_{15}$:

$$\phi^x = (x_4 x_5 (x+1)_0 (x+1)_1 (x+1)_2 (x+1)_3 (x+1)_4 (x+1)_5 (x+2)_0 (x+2)_1).$$

Then, the following sequence of alternating 10-cycles and 4-arcs:

$$\phi^0_+[1_4]\phi^1_-[3_1]\phi^2_+[3_4]\phi^3_-[5_1]\phi^4_+[5_4]\phi^5_-[7_1]\phi^6_+[7_4]\phi^7_-[9_1]\phi^8_+[9_4]\phi^9_-[b_1]\phi^a_+[b_4]\phi^b_-[d_1]\phi^c_+[d_4]\phi^d_-[0_1]\phi^e_+[0_4]$$

may be continued with ϕ^0_-, with opposite orientation to that of the initial ϕ^0_+, where $[x_j]$ stands for a 3-arc starting at the vertex x_j in the previously cited (to the left) oriented 10-cycle. Thus Fos cannot be a $\{\vec{C}_{10}\}_{\vec{P}_5}$-UH digraph. Another way to see this is via the following table of 10-cycles of Fos, where the 10-cycle ϕ_0 intervenes as 10-cycle 0^0:

$$\begin{array}{ll}
0^0{=}(0_4 0_5 1_0 1_1 1_2 1_3 1_4 1_5 2_0 2_1) & 8^0{=}(0_2 0_3 9_2 9_1 7_4 7_5 8_0 8_1 6_4 6_3) \\
1^0{=}(0_0 0_1 0_2 0_3 0_4 2_1 2_2 2_3 2_4 2_5) & 9^0{=}(0_4 0_5 d_0 d_1 d_2 4_3 4_4 4_5 2_0 2_1) \\
2^0{=}(0_3 0_4 0_5 1_0 1_1 1_2 7_3 7_4 9_1 9_2) & a^0{=}(0_4 0_5 d_0 d_1 b_4 b_3 b_2 2_3 2_2 2_1) \\
3^0{=}(0_3 0_4 0_5 d_0 c_5 a_0 9_5 9_4 9_3 9_2) & b^0{=}(0_4 0_5 1_0 3_5 3_4 5_1 5_0 4_5 2_0 2_1) \\
4^0{=}(0_0 0_1 0_2 6_3 6_2 6_1 6_0 5_5 3_0 2_5) & c^0{=}(0_2 0_3 0_4 2_1 2_2 8_3 8_2 8_1 6_4 6_3) \\
5^0{=}(0_4 0_5 1_0 3_5 4_0 4_1 2_4 2_3 2_2 2_1) & d^0{=}(0_3 0_4 2_1 2_0 4_5 5_0 7_5 7_4 9_1 9_2) \\
6^0{=}(0_3 0_4 0_5 1_0 3_5 3_4 3_3 3_2 9_3 9_2) & e^0{=}(0_5 1_0 3_5 4_0 6_5 7_0 9_5 a_0 c_5 d_0) \\
7^0{=}(0_0 0_1 R_2 0_3 9_2 9_3 3_2 3_1 3_0 2_5) & f^0{=}(0_2 0_3 9_2 9_3 3_2 3_3 c_2 c_3 6_2 6_3)
\end{array}$$

where **(a)** hexadecimal notation of integers is used; **(b)** the first 14 10-cycles x^0, ($x = 0, \ldots, 13 = d$), yield corresponding 10-cycles x^j , ($j \in \mathbf{Z}_{15}$). via translation modulo 15 of all indexes; and **(c)** the last two cycles, e^0 and f^0, yield merely additional 10-cycles e^1, e^2, f^1 and f^2 by the same index translation. A corresponding auxiliary table as in the discussions for Pet, Hea and Pap above, in which the $\pm$ assignments are missing and left as an exercise for the reader is as follows:

$$\begin{array}{ll}
0^0{:}(2^0,4^a,1^1,1^e,3^7,2^1,8^9,b^c,b^0,8^8) & 8^0{:}(c^7,d^0,5^7,0^7,0^6,b^4,d^0,c^0,6^6,7^6) \\
1^0{:}(0^e,5^d,c^0,c^9,5^0,0^1,6^e,9^d,9^2,7^0) & 9^0{:}(1^d,4^d,2^c,2^4,3^4,1^2,a^4,b^0,b^c,a^0) \\
2^0{:}(0^e,0^0,7^d,9^3,d^7,c^1,c^7,d^0,9^b,6^0) & a^0{:}(9^b,d^b,5^9,c^b,6^8,7^2,c^9,5^0,d^8,9^0) \\
3^0{:}(6^c,d^8,e^0,5^9,6^9,0^8,6^6,c^9,6^0,9^b) & b^0{:}(6^0,d^b,9^3,0^3,5^0,7^2,d^0,9^0,0^0,5^0) \\
4^0{:}(7^c,c^d,7^6,0^5,7^3,5^2,e^e,d^d,7^0,9^2) & c^0{:}(1^0,2^8,8^8,4^2,a^6,1^6,2^e,8^0,3^6,a^4) \\
5^0{:}(3^6,4^d,b^e,8^b,a^6,1^2,1^0,a^0,8^8,a^0) & d^0{:}(a^4,b^0,4^2,3^7,b^4,a^7,8^0,2^0,2^8,8^9) \\
6^0{:}(3^6,b^0,3^3,1^1,3^9,a^7,f^3,8^9,3^0,2^0) & e^0{:}(3^6,4^2,3^9,4^5,3^c,4^8,3^0,4^b,3^3,4^e) \\
7^0{:}(4^9,a^d,f^3,8^9,4^3,2^2,4^c,b^d,4^0,1^0) & f^0{:}(7^0,6^0,7^3,6^3,7^6,6^6,7^9,6^9,7^c,6^c)
\end{array}$$

Let $A = (A_0, A_1, \ldots, A_g)$, $D = (D_0, D_2, \ldots, D_f)$, $C = (C_0, C_4, \ldots, C_d)$, $F = (F_0, F_8, \ldots, F_9)$ be 4 disjoint 17-cycles. Each $y = A, D, C, F$ has vertices y_i with i expressed as an heptadecimal index up to $g = 16$. We assume that i is advancing in 1,2,4,8 units mod 17, stepwise from left to right, respectively for $y = A, D, C, F$. Then the Biggs-Smith graph B-S is obtained by adding to the disjoint union $A \cup D \cup C \cup F$, for each $i \in \mathbf{Z}_{17}$, a 6-vertex tree T_i formed by the edge-disjoint union of paths $A_iB_iC_i$, $D_iE_iF_i$, and B_iE_i, where the vertices A_i, D_i, C_i, F_i are already present in the cycles A, D, C, F, respectively, and where the vertices B_i and E_i are new and introduced with the purpose of defining the tree T_i, for $0 \leq i \leq g = 16$. Now, $\mathcal{S}$ has the collection $\mathcal{C}_9$ of 9-cycles formed by:

$$\begin{array}{l|l}
S^0{=}(A_0 A_1 B_1 C_1 C_5 C_9 C_d C_0 B_0), & W^0{=}(A_0 A_1 B_1 E_1 F_1 F_9 F_0 E_0 B_0), \\
T^0{=}(C_0 C_4 B_4 A_4 A_3 A_2 A_1 A_0 B_0), & X^0{=}(C_0 C_4 B_4 E_4 D_4 D_2 D_0 E_0 B_0), \\
U^0{=}(E_0 F_0\ F_9 F_1 F_a F_2 E_2 D_2 D_0,) & Y^0{=}(E_0 B_0 A_0 A_1 A_2 B_2 E_2 D_2 D_0), \\
V^0{=}(E_0 D_0 D_2 D_4 D_6 D_8 E_8 F_8 F_0), & Z^0{=}(F_0\ F_8\ E_8 B_8 C_8 C_4 C_0 B_0 E_0),
\end{array}$$

and those 9-cycles obtained from these, as $S^x, \dots, Z^x$, by uniformly adding $x \in \mathbf{Z}_{17}$ mod 17 to all subindexes i of vertices y_i, so that $|\mathcal{C}_9| = 136$.

An auxiliary table presenting the form in which the 9-cycles above share the vertex sets of 3-arcs, either O-O or not, is shown below, in a fashion similar to those above for Pet, Hea, Pap and Fos, where minus signs are set but plus signs are tacit now:

S^0:($-T_1^e, T_7^1, -Z_4^1, S_4^d, S_3^4, -Z_3^9, T_0^d, -T_6^0, U_8^0$),	W^0:($-U_4^0, W_2^8, W_1^9, -U_3^1, X_7^2, -X_4^b, Y_6^0, -X_8^0, X_5^9$),
T^0:($S_6^4, -S_0^3, -Y_2^2, T_4^1, T_3^g, -Y_1^0, -S_7^0, S_1^g, V_8^0$),	X^0:($-V_4^0, X_2^f, X_1^2, -V_3^4, -W_5^6, W_8^8, -Z_8^0, W_4^f, -W_7^0$),
U^0:($Y_3^g, -U_6^1, Z_7^1, -W_3^g, -W_0^0, Z_0^9, -U_1^g, Y_0^0, S_8^0$),	Y^0:($U_7^0, -T_5^0, -T_2^f, U_0^1, -Y_8^2, V_2^f, W_6^0, V_5^0, -Y_4^f$),
V^0:($-Z_2^d, -V_6^4, Y_5^2, -X_3^d, -X_0^0, Y_7^0, -V_1^d, -Z_5^0, T_8^0$),	Z^0:($U_5^8, -Z_6^8, -V_0^4, -S_5^8, -S_2^g, -V_7^0, -Z_1^9, U_2^g, -X_6^0$),

This table is extended by adding $x \in \mathbf{Z}_{17}$ uniformly mod 17 to all superindexes, confirming that B-S is not $\{\vec{C}_9\}_{\vec{P}_4}$-UH.. □

4 Separator digraphs of 7 CDT graphs

For each of the 7 CDT graphs G that are $\{\vec{C}_g\}_{\vec{P}_k}$-UH digraphs according to Theorem 3, the following construction yields a corresponding digraph $\mathcal{S}(G)$ of outdegree and indegree two and having underlying cubic graph structure and the same automorphism group of G. The vertices of $\mathcal{S}(G)$ are defined as the $(k-1)$-arcs of G. We set an arc in $\mathcal{S}(G)$ from each vertex $a_1a_2\dots a_{k-1}$ into another vertex $a_2\dots a_{k-1}a_k$ whenever there is an oriented g-cycle $(a_1a_2\dots a_{k-1}a_k\dots)$ in the $\{\eta\vec{C}_g\}_{\vec{P}_k}$-OOC provided by Theorem 3 to G. Thus each oriented g-cycle in the mentioned $\{\eta\vec{C}_g\}_{\vec{P}_k}$-OOC yields an oriented g-cycle of $\mathcal{S}(G)$. In addition we set an edge e in $\mathcal{S}(G)$ for each transposition of a $(k-1)$-arc of G, say $h = a_1a_2\dots a_{k-1}$, taking it into $h^{-1} = a_{k-1}a_{k-2}\dots a_1$. Thus the ends of e are h and h^{-1}. As usual, the edge e is considered composed by two O-O arcs.

The polyhedral graphs G here are the tetrahedral graph $G = K_4$, the 3-cube graph $G = Q_3$ and the dodecahedral graph $G = \Delta$. The corresponding graphs $\mathcal{S}(G)$ have their underlying graphs respectively being the truncated-polyhedral graphs of the corresponding dual-polyhedral graphs that we can refer as the truncated tetrahedron, the truncated octahedron and the truncated icosahedron. In fact:

(A) $\mathcal{S}(K_4)$ has vertices $01, 02, 03, 12, 13, 23, 10, 20, 30, 21, 31, 32$; the cycles (123), (210), (301), (032) of the $\{\eta\vec{C}_g\}_{\vec{P}_k}$-OOC of K_4 give place to the oriented 3-cycles $(12, 23, 31)$, $(21, 10, 02)$, $(30, 01, 13)$, $(03, 32, 20)$ of $\mathcal{S}(K_4)$; the additional edges of $\mathcal{S}(K_4)$ are $(01, 10)$, $(02, 20)$, $(03, 30)$, $(12, 21)$, $(13, 31)$, $(23, 32)$.

(B) The of oriented cycles of $\mathcal{S}(Q_3)$ corresponding to the $\{\eta\vec{C}_g\}_{\vec{P}_k}$-OOC of Q_3 are $(01, 13, 32, 20)$, $(10, 04, 45, 51)$, $(31, 15, 57, 73)$,$(23, 37, 76, 62)$, $(02, 26, 64, 40)$, $(46, 67, 75, 54)$; the additional edges of $\mathcal{S}(Q_3)$ are $(01, 10)$, $(23, 32)$, $(45, 54)$, $(67, 76)$, $(02, 20)$, $(13, 31)$, $(46, 64)$, $(57, 75)$, $(04, 40)$, $(15, 51)$, $(26, 62)$, $(37, 73)$.

(C) The oriented cycles of $\mathcal{S}(\Delta)$ corresponding to the $\{\eta\vec{C}_g\}_{\vec{P}_k}$-OOC of Δ are $(a_0a_1, a_1a_2, a_2a_3, a_3a_4, a_4\ a_0)$, $(c_4c_3, c_3c_2, c_2c_1, c_1c_0, c_0c_4)$, and both $(a_xd_x, d_xb_{x-2}, b_{x-2}d_{x+1}, d_{x+1}\ a_{x+1}, a_{x+1}a_x)$ and $(d_xb_{x+2}, b_{x+2}c_{x+2}, c_{x+2}c_{x-2}, c_{x-2}b_{x-2}, b_{x-2}d_x)$, for each $x \in \mathbf{Z}_5$;

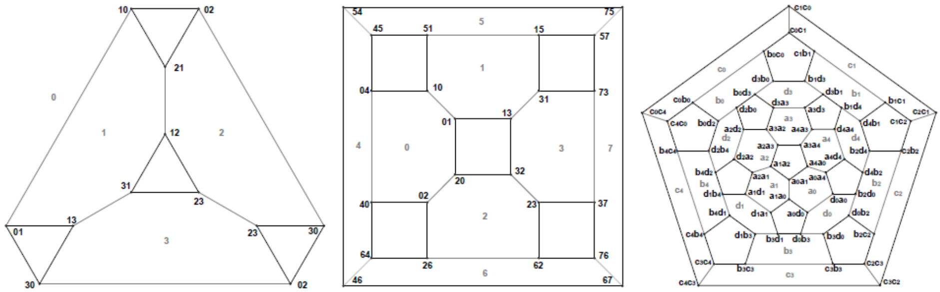

Figure 1: $\mathcal{S}(K_4)$, $\mathcal{S}(Q_3)$ and $\mathcal{S}(\Delta)$

the additional edges are $(a_xa_{x+1}, a_{x+1}a_x)$, $(c_xc_{x+1}, c_{x+1}c_x)$, $(a_xd_x, d_x\ a_x)$, $(d_xb_{x+2}, b_{x+2}d_x)$, $(b_xd_{x+2}, d_{x+2}b_x)$, and (b_xc_x, c_xb_x), for each $x \in \mathbf{Z}_5$.

Among the 7 CDT graphs G that are $\{\vec{C}_g\}_{\vec{P}_k}$-UH digraphs, the polyhedral graphs treated above are exactly those having arc-transitivity $k = 2$. Figure 1 contains representations of these graphs $\mathcal{S}(G)$, namely $\mathcal{S}(K_4)$, $\mathcal{S}(Q_3)$ and $\mathcal{S}(\Delta)$, with the respective 3-cycles, 4-cycles and 5-cycles in black trace to be considered clockwise oriented, but for the external cycles in the cases $\mathcal{S}(Q_3)$ and $\mathcal{S}(\Delta)$, to be considered counterclockwise oriented. The remaining edges (to be referred as transposition edges) are gray colored and considered bidirectional. The cycles having alternate black and gray edges here, arising respectively from arcs from the oriented cycles and from the transposition edges, are 6-cycles. Each such 6-cycle has its vertices sharing the notation, indicated in gray, of a unique vertex of the corresponding G. Each vertex of G is used as such gray 6-cycle indication.

The truncated tetrahedron, truncated octahedron and truncated icosahedron, oriented as indicated for Figure 1, are the Cayley digraphs of the groups A_4, S_4 and A_5, with respective generating sets $\{(123), (12)(34)\}$, $\{(1234), (12)\}$ and $\{(12345), (23)(45)\}$. Thus

$$\mathcal{S}(K_4)\equiv Cay(A_4,\{(123),(12)(34)\}),\mathcal{S}(Q_3)\equiv Cay(S_4,\{(1234),(12)\}),\mathcal{S}(\Delta)\equiv Cay(A_5,\{(12345),(23)(45)\}).$$

(D) The oriented cycles of $\mathcal{S}(K_{3,3})$ corresponding to the $\{\eta\vec{C}_g\}_{\vec{P}_k}$-OOC of $K_{3,3}$ are:

$$\begin{array}{lll}(123, 234, 341, 412), & (321, 210, 103, 032), & (432, 325, 254, 543),\\ (143, 430, 301, 014), & (214, 145, 452, 521), & (012, 125, 250, 501),\\ (523, 230, 305, 052), & (034, 345, 450, 503), & (541, 410, 105, 054);\end{array}$$

and additional edges of $\mathcal{S}(K_{3,3})$ are:

$$\begin{array}{l}(123, 321), (234, 432), (341, 143), (412, 214), (210, 012), (103, 301),\\ (032, 230), (325, 523), (254, 452), (543, 345), (430, 034), (014, 410),\\ (145, 541), (521, 125), (250, 052), (501, 105), (305, 503), (450, 054).\end{array}$$

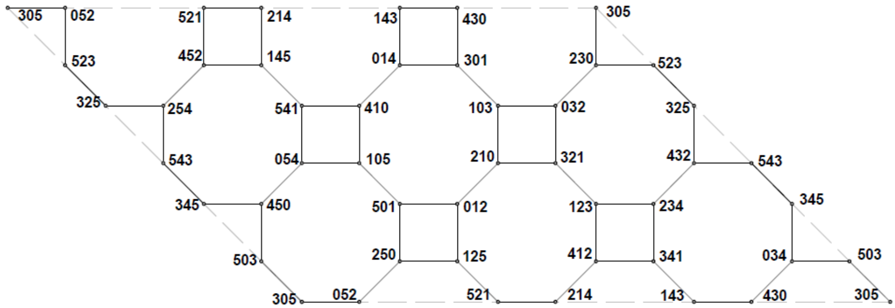

Figure 2: $\mathcal{S}(K_{3,3})$

A cut-out toroidal representation of $\mathcal{S}(K_{3,3})$ is in Figure 2, where black-traced 4-cycles are considered oriented clockwise, corresponding to the oriented 4-cycles in the $\{\eta\vec{C}_g\}_{\vec{P}_k}$-OOC of $K_{3,3}$, and where gray edges represent transposition edges of $\mathcal{S}(K_{3,3})$, which gives place to the alternate 8-cycles, constituted each by an alternation of 4 transposition edges and 4 arcs of the oriented 4-cycles. In $\mathcal{S}(K_{3,3})$, there are 9 4-cycles and 9 8-cycles. Now, the group $<(0,5,4,1)(2,3),(0,2)(1,5)>$ has order 36 and acts regularly on the vertices of $\mathcal{S}(K_{3,3})$. For example, $(0,2)(1,5)$ stabilizes the edge $(145, 541)$, and the permutation $(0,5,4,1)(2,3)$ permutes (clockwise) the black oriented 4-cycle $(541, 410, 105, 054)$. Thus $\mathcal{S}(K_{3,3})$ is a Cayley digraph. Also, observe the oriented 9-cycles in $\mathcal{S}(K_{3,3})$ obtained by traversing alternatively 2-arcs in the oriented 4-cycles and transposition edges; there are 6 such oriented 9-cycles.

(E) The collection of oriented cycles of $\mathcal{S}(Des)$ corresponding to the $\{\eta\vec{C}_g\}_{\vec{P}_k}$-OOC of Des is formed by the following oriented 6-cycles, where $x \in \mathbf{Z}_5$:

$$\begin{array}{l}
(x_0x_1x_2,\ x_1x_2x_3,\ x_2x_3x_0^1,\ x_3x_0^1x_3^4,\ x_0^1x_3^4x_0,\ x_3^4x_0x_1),\\
(x_1x_0x_3^4,\ x_0x_3^4x_2^4,\ x_3^4x_2^4x_1^2,\ x_2^4x_1^2x_2^2,\ x_1^2x_2^2x_1,\ x_2^2x_1x_0),\\
(x_2x_1x_0,\ x_1x_0x_3^3,\ x_0x_3^3x_2^3,\ x_3^3x_2^3x_1^3,\ x_2^3x_1^3x_2,\ x_1^3x_2x_1),\\
(x_0x_3^4x_0^1,\ x_3^4x_0^1x_1^1,\ x_0^1x_1^1x_2^3,\ x_1^1x_2^3x_3^3,\ x_2^3x_3^3x_0,\ x_3^3x_0x_3^4),
\end{array}$$

respectively for the 6-cycles A^x, B^x, C^x, D^x, where x_i^j stands for $(x+j)_i$; each of the participant vertices here is an end of a transposition edge. Figure 3 represents a subgraph $\mathcal{S}(M_3)$ of $\mathcal{S}(Des)$ associated with the matching M_3 of Des indicated in its representation "inside" the left-upper "eye" of the figure, where vigesimal integer notation is used (up to $j = 19$); in the figure, additional intermittent edges were added that form 12 square pyramids, 4 such edges departing from a corresponding extra vertex; so, 12 extra vertices appear that can be seen as the vertices of a cuboctahedron whose edges are 3-paths with inner edge in $\mathcal{S}(M_3)$ and intermittent outer edges. There is a total of 5 matchings, like M_3, that we denote M_x, where $x = 3, 7, b, f, j$. In fact, $\mathcal{S}(Des)$ is obtained as the union $\bigcup\{\mathcal{S}(M_x); x = 3, 7, b, f, j\}$. Observe that the components of the subgraph induced by the matching M_x in Des are at mutual distance 2 and that M_x can be divided into three pairs of edges with the ends of each pair at minimum distance 4, facts that can be used to establish the properties of $\mathcal{S}(Des)$.

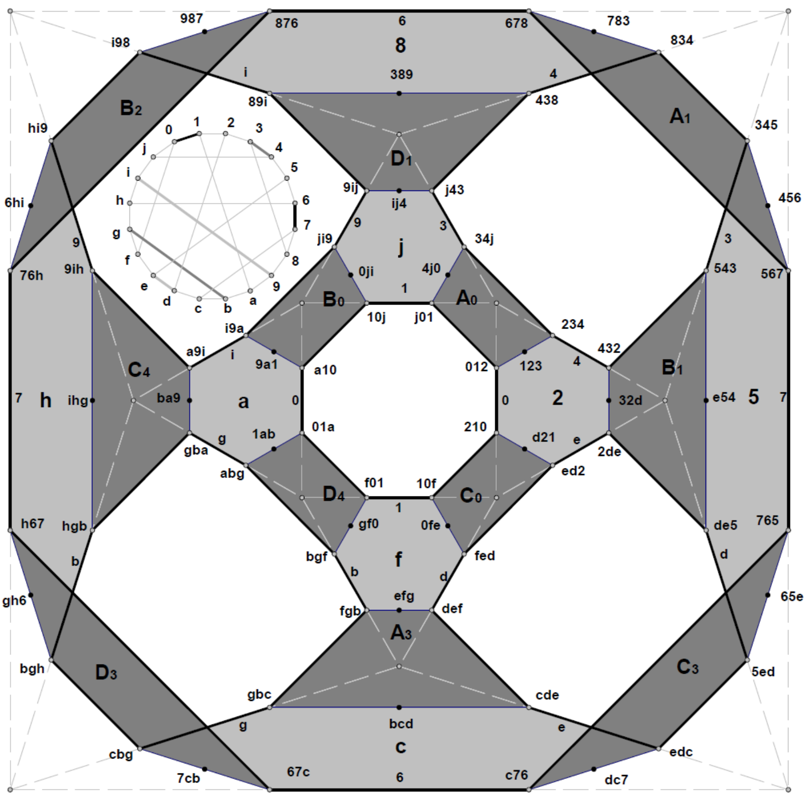

Figure 3: M_3 and the subgraph of $\mathcal{S}(Des)$ associated to it

In Figure 3 there are: 12 oriented 6-cycles (dark-gray interiors); 6 alternate 8-cycles (thick-black edges); and 8 9-cycles with alternate 2-arcs and transposition edges (light-gray interiors). The 6-cycles are denoted by means of the associated oriented 6-cycles of Des. Each 9-cycle has its vertices sharing the notation of a vertex of $V(Des)$ and this is used to denote it. Each edge e in M_3 has associated a closed walk in Des containing every 3-path with central edge e; this walk can be used to determine a unique alternate 8-cycle in $\mathcal{S}(M_3)$, and viceversa. Each 6-cycle has two opposite (black) vertices of degree two in $\mathcal{S}(M_3)$. In all, $\mathcal{S}(Des)$ contains 120 vertices; 360 arcs amounting to 120 arcs in oriented 6-cycles and 120 transposition edges; 20 dark-gray 6-cycles; 30 alternate 8-cycles; and 20 light-gray 9-cycles. By filling the 6-cycles and 8-cycles here with 2-dimensional faces, then the 120 vertices, 180 edges (of the underlying cubic graph) and resulting $20 + 30 = 50$ faces yield a surface of Euler characteristic $120 - 180 + 50 = -10$, so this surface genus is 6. The automorphism group of Des is $G = S_5 \times \mathbf{Z}_2$. Now, G contains three subgroups of index 2: two isomorphic to to S_5 and one isomorphic to $A_5 \times \mathbf{Z}_2$. One of the two subgroups of G isomorphic to S_5 (the diagonal copy) acts regularly on the vertices of $\mathcal{S}(Des)$ and hence $\mathcal{S}(Des)$ is a Cayley digraph.

(F) The collection of oriented cycles of $\mathcal{S}(Cox)$ corresponding to the $\{\eta\vec{C}_g\}_{\vec{P}_k}$-OOC of Cox is formed by oriented 7-cycles, such as:

$$\underline{0^1} = (u_1u_2u_3, u_2u_3u_4, u_3u_4u_5, u_4u_5u_6, u_5u_6u_0, u_6u_0u_1, u_0u_1u_2),$$

and so on for the remaining oriented 7-cycles $\underline{x^y}$ with $x \in \{0, \ldots, 7\}$ and $y \in \{1, 2, 3\}$, based on the corresponding table in the proof of Theorem 3. Moreover, each vertex of $\mathcal{S}(Cox)$ is adjacent via a transposition edge to its reversal vertex. Thus $\mathcal{S}(Cox)$ has: underlying cubic graph; indegree = outdegree = 2; 168 vertices; 168 arcs in 24 oriented 7-cycles; 84 transposition edges; and 42 alternate 8-cycles. Its underlying cubic graph has 252 edges. From this information, by filling the 7- and 8-cycles mentioned above with 2-dimensional faces, we obtain a surface with Euler characteristic $168 - 252 + (24 + 42) = -18$, so its genus is 10. On the other hand, $\mathcal{S}(Cox)$ is the Cayley digraph of the automorphism group of the Fano plane, namely $PSL(2, 7) = GL(3, 2)$ [4], of order 168, with a generating set of two elements, of order 2 and 7, representable by the 3×3-matrices $(100, 001, 010)^T$ and $(001, 101, 010)^T$ over the field F_2, where T stands for transpose.

Figure 4 depicts a subgraph of $\mathcal{S}(Cox)$ containing in its center a (twisted) alternate 8-cycle that we denote (in gray) z_1u_1, and, around it, four oriented 7-cycles adjacent to it, (namely $\underline{1^1}$, $\underline{7^1}$, $\underline{2^3}$, $\underline{6^3}$, denoted by their corresponding oriented 7-cycles in Cox, also in gray), plus four additional oriented 7-cycles (namely $\underline{0^0}$, $\underline{3^2}$, $\underline{4^1}$, $\underline{5^2}$), related to four 9-cycles mentioned below. Black edges represent arcs, and the orientation of these 8 7-cycles is taken clockwise, with only gray edges representing transposition edges of $\mathcal{S}(Cox)$. Each edge of Cox determines an alternate 8-cycle of $\mathcal{S}(Cox)$. In fact, Figure 4 contains not only the alternate 8-cycle corresponding to the edge z_1u_1 mentioned above, but also those corresponding to the edges u_1u_2, v_1z_1, t_1z_1 and u_0u_1. These 8-cycles and the 7-cycles in the figure show that alternate 8-cycles C and C' adjacent to a particular alternate 8-cycle C'' in $\mathcal{S}(Cox)$ on opposite edges e and e' of C'' have the same opposite edge e'' both to e and e' in C and C', respectively. There are two instances of this property in Figure 4, where the two edges taking the place of e'' are the large central diagonal gray ones, with C'' corresponding to u_1z_1. As in (E) above, the fact that each edge e of Cox determines

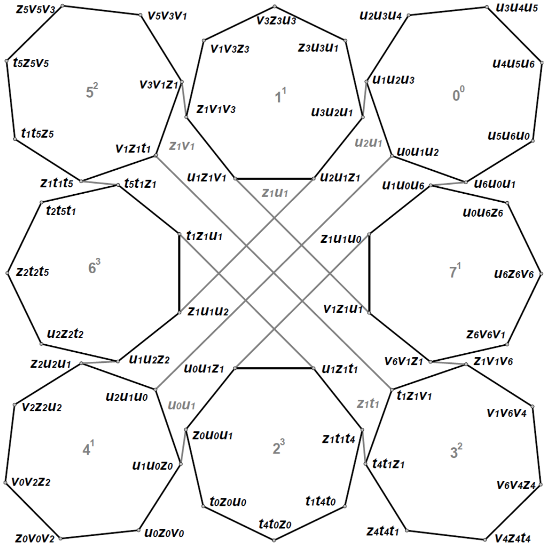

Figure 4: A subdigraph of $\mathcal{S}(Cox)$ associated with an edge of Cox

an alternate 8-cycle of $\mathcal{S}(Cox)$ is related with the closed walk that covers all the 3-paths having e as central edge, and the digraph $\mathcal{S}(Cox)$ contains 9-cycles that alternate 2-arcs in the oriented 7-cycles with transposition edges. In the case of Figure 4, these 9-cycles are, in terms of the orientation of the 7-cycles:

$$(u_2u_1z_1,\, u_1z_1v_1,\, z_1v_1v_3,\, v_3v_1z_1,\, v_1z_1t_1,\, z_1t_1t_5,\, t_5t_1z_1,\, t_1z_1u_1,\, z_1u_1u_2),$$
$$(v_1z_1u_1, z_1u_1u_0, u_1u_0u_6, u_6u_0u_1, u_0u_1u_2, u_1u_2u_3, u_3u_2u_1, u_2u_1z_1, u_1z_1v_1),$$
$$(u_0u_1z_1,\, u_1z_1t_1,\, z_1t_1t_4,\, t_4t_1z_1,\, t_1z_1v_1,\, z_1v_1v_6,\, v_6v_1z_1,\, v_1z_1u_1,\, z_1u_1u_0),$$
$$(t_1z_1u_1, z_1u_1u_2, u_1u_2z_2, z_2u_2u_1, u_2u_1u_0, u_1u_0z_0, z_0u_0u_1, u_0u_1z_1, u_1z_1t_1).$$

A convenient description of alternate 8-cycles, as those denoted in gray in Figure 4 by the edges $z_1u_1, z_1v_1, u_2u_1, u_0u_1, z_1t_1$ of Cox, is given by indicating the successive passages through arcs of the oriented 7-cycles, with indications by means of successive subindexes in the order of presentation of their composing vertices, which for those 5 alternate 8-cycles looks like:

$$(1^1_{60}, 7^1_{56}, 2^3_{60}, 6^3_{56}), \quad (5^2_{12}, 3^2_{23}, 7^1_{45}, 1^1_{01}), \quad (0^1_{01}, 1^1_{56}, 6^3_{60}, 4^1_{56}), \quad (2^3_{56}, 7^1_{60}, 0^0_{56}, 4^1_{60}), \quad (3^2_{12}, 5^2_{23}, 6^3_{45}, 2^3_{01}).$$

In a similar fashion, the four bi-alternate 9-cycles displayed just above can be presented by means of the shorter expressions:

$$(1^1_{61}, 5^2_{13}, 6^3_{46}), \quad (7^1_{50}, 0^1_{50}, 1^1_{50}), \quad (2^3_{61}, 3^2_{13}, 7^1_{46}), \quad (6^3_{50}, 4^1_{50}, 2^3_{50}).$$

By the same token, there are twenty four tri-alternate 28-cycles, one of which is expressible as:

$$(0^1_{03}, 6^1_{03}, 3^2_{40}, 2^3_{36}, 5^3_{36}, 4^2_{62}, 1^1_{40}).$$

At this point, we observe that $\mathcal{S}(K_4)$, $\mathcal{S}(Q_3)$ and $\mathcal{S}(\Delta)$ have alternate 6-cycles, while $\mathcal{S}(K_{3,3})$, $\mathcal{S}(Des)$ and $\mathcal{S}(Cox)$ have alternate 8-cycles.

(G) The collection of oriented cycles of $\mathcal{S}(Tut)$ corresponding to the $\{\eta\vec{C}_g\}_{\vec{P}_k}$-OOC of Tut is formed by oriented 8-cycles, such as: $\underline{A^0} =$

$$(4_50_00_10_20_3, 0_00_10_20_30_4, 0_10_20_30_40_5, 0_20_30_40_51_0, 0_30_40_51_04_5, 0_40_51_04_50_0, 0_51_04_50_00_1, 1_04_50_00_10_2)$$

and so on for the remaining oriented 8-cycles $\underline{X^y}$ with $X \in \{A, \ldots, R\}$ and $y \in \mathbf{Z}_5$ based on the corresponding table in the proof of Theorem 3. Moreover, each vertex of $\mathcal{S}(Tut)$ is adjacent via a transposition edge to its reversal vertex. Thus $\mathcal{S}(Tut)$ has: underlying cubic graph; indegree = outdegree = 2; 720 vertices; 720 arcs in 90 oriented 8-cycles; 360 transposition edges; and 180 alternate 8-cycles, (36 of which are displayed below); its underlying cubic graph has 1080 edges. From this information, by filling the 900 8-cycles above with 2-dimensional faces, a surface with Euler characteristic $720 - 1080 + 240 = -120$ is obtained, so genus = 61. On the other hand, the automorphism group of Tut is the projective semilinear group $G = P\Gamma L(2, 9)$ [13], namely the group of collineations of the projective line $PG(1, 9)$. The group G contains exactly three subgroups of index 2 (and so of order 720), one of which (namely M_{10}, the Mathieu group of order 10, acts regularly on the vertices of $\mathcal{S}(Tut)$. Thus $\mathcal{S}(Tut)$ is a Cayley digraph.

A fifth of the 180 alternate 8-cycles of $\mathcal{S}(Tut)$ can be described by presenting in each case the successive pairs of vertices in each oriented 8-cycle $\underline{X^y}$ as follows, each such pair denoted by means of the notation $X^y_{u(u+1)}$, where u stands for the 4-arc in position u in $\underline{X^y}$, with 0 indicating the first position:

$(A^0_{01},$	$M^0_{34},$	$B^4_{34},$	$K^0_{12})$	$(A^0_{12},$	$P^1_{01},$	$I^0_{70},$	$M^0_{23})$	$(A^0_{23},$	$H^0_{34},$	$B^1_{70},$	$P^1_{70})$
$(A^0_{34},$	$J^0_{70},$	$L^3_{70},$	$H^0_{23})$	$(A^0_{45},$	$E^0_{70},$	$P^0_{45},$	$J^0_{67})$	$(A^0_{56},$	$E^1_{45},$	$F^1_{70},$	$E^0_{67})$
$(A^0_{67},$	$G^0_{45},$	$M^1_{67},$	$E^1_{34})$	$(A^0_{70},$	$K^0_{23},$	$L^2_{12},$	$G^0_{34})$	$(B^0_{01},$	$C^2_{34},$	$Q^3_{23},$	$P^0_{67})$
$(B^0_{12},$	$R^3_{34},$	$N^1_{56},$	$C^2_{23})$	$(B^0_{23},$	$M^1_{45},$	$Q^2_{67},$	$R^3_{23})$	$(B^0_{45},$	$D^3_{67},$	$R^1_{70},$	$K^1_{01})$
$(B^0_{56},$	$D^0_{34},$	$O^0_{56},$	$D^3_{56})$	$(B^0_{67},$	$H^4_{45},$	$C^4_{67},$	$D^0_{23})$	$(C^0_{01},$	$G^3_{70},$	$H^3_{70},$	$M^0_{01})$
$(C^0_{12},$	$N^4_{67},$	$F^3_{45},$	$G^3_{67})$	$(C^0_{45},$	$L^0_{67},$	$J^2_{01},$	$Q^1_{12})$	$(C^0_{56},$	$H^0_{56},$	$O^4_{34},$	$L^0_{56})$
$(C^0_{70},$	$M^0_{12},$	$I^0_{01},$	$D^1_{12})$	$(D^0_{01},$	$I^4_{12},$	$O^1_{12},$	$I^3_{56})$	$(D^0_{45},$	$O^2_{67},$	$L^1_{45},$	$O^0_{45})$
$(D^0_{70},$	$I^3_{67},$	$P^4_{12},$	$R^3_{67})$	$(E^0_{01},$	$N^4_{01},$	$K^1_{45},$	$P^0_{34})$	$(E^0_{12},$	$N^2_{34},$	$F^3_{34},$	$N^4_{70})$
$(E^0_{23},$	$M^0_{70},$	$H^3_{01},$	$N^2_{23})$	$(E^0_{56},$	$F^1_{01},$	$Q^2_{45},$	$F^0_{67})$	$(F^0_{12},$	$J^3_{56},$	$P^3_{56},$	$Q^1_{34})$
$(F^0_{23},$	$N^4_{45},$	$R^1_{45},$	$J^3_{45})$	$(F^0_{56},$	$Q^2_{56},$	$M^1_{56},$	$G^0_{56})$	$(G^0_{01},$	$I^1_{45},$	$O^4_{23},$	$H^0_{67})$
$(G^0_{12},$	$Q^1_{01},$	$J^2_{12},$	$I^1_{34})$	$(G^0_{23},$	$L^2_{23},$	$R^2_{12},$	$Q^1_{70})$	$(H^0_{12},$	$L^3_{01},$	$K^1_{34},$	$N^4_{12})$
$(I^0_{23},$	$J^1_{23},$	$K^1_{67},$	$O^2_{01})$	$(J^0_{34},$	$R^3_{56},$	$P^4_{23},$	$K^0_{56})$	$(K^0_{70},$	$R^0_{01},$	$L^0_{34},$	$O^1_{70})$

Again, as in the previously treated cases, we may consider the oriented paths that alternatively traverse two arcs in an oriented 8-cycle and then a transposition edge, repeating this operation until a closed path is formed. It happens that all such bi-alternate cycles are 12-cycles. For example with a notation akin to the one in the last table, we display the first row of the corresponding table of 12-cycles:

$(A^0_{02},$	$P^1_{02},$	$R^0_{60},$	$K^0_{02})$	$(A^0_{13},$	$H^0_{35},$	$C^0_{60},$	$M^0_{13})$	$(A^0_{24},$	$J^0_{71},$	$Q^4_{13},$	$P^1_{60})$
(......,	......,	......,	......)	(......,	......,	......,	......)	(......,	......,	......,	......)

As in the case of the alternate 8-cycles above, which are 180, there are 180 bi-alternate 12-cycles in $\mathcal{S}(Tut)$. On the other hand, an example of a tri-alternate 32-cycle in $\mathcal{S}(Tut)$ is given by:

$$(A^0_{03}, \quad H^0_{36}, \quad O^4_{36}, \quad D^2_{50}, \quad I^0_{61}, \quad D^1_{14}, \quad O^1_{50}, \quad K^0_{72}).$$

There is a total of 90 such 32-cycles. Finally, an example of a tetra-alternate 15-cycle in $\mathcal{S}(Tut)$ is given by $(A^0_{04}, J^0_{73}, K^0_{62})$, and there is a total of 240 such 15-cycles. More can be said about the relative structure of all these types of cycles in $\mathcal{S}(Tut)$.

The automorphism groups of the graphs $\mathcal{S}(G)$ in items (A)-(G) above coincide with those of the corresponding graphs G because the construction of $\mathcal{S}(G)$ depends solely on the structure of G as analyzed in Section 3 above. Salient properties of the graphs $\mathcal{S}(G)$ are contained in the following statement.

Theorem 4.1. For each CDT graph that is a $\{\vec{C}_g\}_{\vec{P}_k}$-UH digraph, $\mathcal{S}(G)$ is: **(a)** a vertex-transitive digraph with indegree $=$ outdegree $= 2$, underlying cubic graph and the automorphism group of G; **(b)** a $\{\vec{C}_g, \vec{C}_2\}$-ultrahomogeneous digraph, where $\vec{C}_g$ stands for oriented g-cycle coincident with its induced subdigraph and each vertex is the intersection of exactly one such $\vec{C}_g$ and one $\vec{C}_2$; **(c)** a Cayley digraph. Moreover, the following additional properties hold, where $s(G) =$ subjacent undirected graph of $\mathcal{S}(G)$:

(A) $\mathcal{S}(K_4) \equiv Cay(A_4, \{(123), (12)(34)\})$, $s(K_4) =$ truncated octahedron;

(B) $\mathcal{S}(Q_3) \equiv Cay(S_4, \{(1234), (12)\})$, $s(Q_3) =$ truncated octahedron;

(C) $\mathcal{S}(\Delta) \equiv Cay(A_5, \{(12345), (23)(45)\})$, $s(\Delta) =$ truncated icosahedron;

(D) $\mathcal{S}(K_{3,3})$ is the Cayley digraph of the subgroup of S_6 on the vertex set $\{0, 1, 2, 3, 4, 5\}$ generated by $(0, 5, 4, 1)(2, 3)$ and $(0, 2)(1, 5)$ and has a toroidal embedding whose faces are delimited by 9 oriented 4-cycles and 9 alternate 8-cycles;

(E) $\mathcal{S}(Des)$ is the Cayley digraph of a diagonal copy of S_5 in the automorphism group $S_5 \times \mathbf{Z}_2$ of Des and has a 6-toroidal embedding whose faces are delimited by 20 oriented 6-cycles and 30 alternate 8-cycles;

(F) $\mathcal{S}(Cox) \equiv Cay(GL(3, 2), \{(100, 001, 010)^T, (001, 101, 010)^T\})$, has a 10-toroidal embedding whose faces are delimited by 24 oriented 7-cycles and 42 alternate 8-cycles;

(G) $\mathcal{S}(Tut)$ is the Cayley digraph of a subgroup M_{10} of order 2 in the automorphism group $P\Gamma L(2, 9)$ of Tut and has a 61-toroidal embedding whose faces are delimited by 90 oriented 8-cycles and 180 alternate 8-cycles.

Corollary 4.2. The bi-alternate cycles in the graphs $\mathcal{S}(G)$ above are 9-cycles unless either $G = Q_3$ or $G = \Delta$, in which cases they are respectively 12-cycles and 15-cycles.

Acknowledgement

The author is grateful to the referee of a previous version of this paper for indications and corrections that lead to the present manuscript and for encouragement with respect to the value of the construction of the 7 directed graphs $\mathcal{S}(G)$ in Section 4.

References

[1] N. L. Biggs, Algebraic Graph Theory (2nd ed.), Cambridge University Press, 1993.

[2] B. Mohar and C. Thomassen, Graphs on surfaces, Johns Hopkins Univ. Press, 2001.

[3] A. E. Brouwer, A. M. Cohen and A. Neumaier, *Distance–Regular Graphs*, Springer-Verlag, New York 1989.

[4] E. Brown and N. Loehr, Why is $PSL(2,7) = GL(3,2)$?, *Amer. Math. Mo.* **116-8** (2009), 727–732.

[5] P. J. Cameron, 6-transitive graphs, *J. Combin. Theory Ser. B* **28** (1980), 168–179.

[6] G. L. Cherlin, The Classification of Countable Homogeneous Directed Graphs and Countable Homogeneous n-tournaments, *Memoirs Amer. Math. Soc.*, vol. 131, number 612, Providence RI, January 1988.

[7] A. Devillers, *Classification of some homogeneous and ultrahomogeneous structures*, Dr. Sc. Thesis, Université Libre de Bruxelles, 2001–2002.

[8] R. Fraïssé, Sur l'extension aux relations de quelques proprietés des ordres, *Ann. Sci. École Norm. Sup.* **71** (1954), 363–388.

[9] A. Gardiner, Homogeneous graphs, *J. Combin. Theory Ser. B* **20** (1976), 94–102.

[10] C. Godsil and G. Royle, *Algebraic Graph Theory*, Springer–Verlag, 2001.

[11] Ja. Ju. Gol'fand and M. H. Klin, On k-homogeneous graphs, *Algorithmic studies in combinatorics* **186** (1978), 76–85, in Russian.

[12] J. L. Gross and T. W. Tucker, *Topological Graph Theory*, Wiley Interscience, 1987.

[13] J. W. P. Hirschfeld, *Projective Geometries over Finite Fields*, Oxford Science Publications, 2nd ed., Clarendom Press, Oxford 1998.

[14] D. C. Isaksen, C. Jankowski and S. Proctor, On K_*-ultrahomogeneous graphs, *Ars Combinatoria* **82** (2007), 83–96.

[15] I. A. Faradzev, A. A. Ivanov, M. Klin et al., The Algebraic Theory of Combinatorial Objects, *Math. Appl.* (Soviet Series), 84, Dordrecht, Kluwer, 1992.

[16] A. H. Lachlan and R. Woodrow, Countable ultrahomogeneous undirected graphs, *Trans. Amer. Math. Soc.* **262** (1980), 51–94.

[17] C. Ronse, On homogeneous graphs, *J. London Math. Soc.* **17** (1978), 375–379.

[18] B. I. Rose and R. E. Woodrow, Ultrahomogeneous structures, *Mathematical Logic Quarterly* **27** (1981), 23–30.

[19] J. Sheehan, Smoothly embeddable subgraphs, *J. London Math. Soc.* **9** (1974), 212–218.

[20] A. T. White, *Graphs of groups on surfaces*, North-Holland, Mathematics Studies 188, 2001.